Article

Quantum path integral for financial options

Lester Ingber[1,†,‡]

[1] Lester Ingber Research; ingber@alumni.caltech.edu [1]
† Current address: Lester Ingber Research, Ashland, OR, USA

Received: date; Accepted: date; Published: date

Abstract: A quantum path-integral algorithm qPATHINT has expanded classical PATHINT, from 1 to N dimensions, and from classical to quantum systems. Classical PATHINT demonstrated development of Eurodollar options in industrial applications. **Method**: qPATHINT is developed using mathematical-physics methods of path integrals in quantum spaces. Studies using supercomputer resources have tested various dimensions for their scaling limits. All Greeks for options trading are calculated in quantum-money spaces. **Results**: A 2-dimensional model of Eurodollar volatility of volatility, previously calculated using PATHINT, has been calculated using qPATHINT. A 3-dimensional path-integral propagation of qPATHINT for both systems is within normal computational bounds on supercomputers. **Conclusion**: The mathematical-physics and computer parts of the study are successful, in that 2-dimensional and 3-dimensional calculations are demonstrated to be feasible.

Keywords: path integral; quantum mechanics; financial options, supercomputer

---

Funding: The author thanks the Extreme Science and Engineering Discovery Environment (XSEDE.org), for supercomputer grants since February 2013, starting with Electroencephalographic field influence on calcium momentum waves, one under PHY130022 and two under TG-MCB140110. The current grant under TG-MCB140110, Quantum path-integral qPATHTREE and qPATHINT algorithms, was started in 2017, and renewed through December 2018.

1. Introduction

There is a long list of governments and companies developing hardware and software for quantum computing. A recent list includes:

D-WAVE (Canada)
DeepMind (Canada)
Facebook
Google
IBM
Intel
Microsoft
National Laboratory for Quantum Information Sciences (China)
Nippon Telegraph and Telephone
NOKIA Bell Labs
NSA
Post-Quantum
Rigetti
Russian Quantum Center
Toshiba
Quantum Circuits
Quantum Technologies (European Union)

Since error correction is a vital consideration for quantum computers, this is a major task being addressed.

It is inevitable that these developments in quantum hardware and software will spin off into all levels of schools and post-education, and eventually products and services based on quantum processes will be offered for general consumption. Then, it is a small step forward to appreciate that some new quantum products will require calculations using quantum variables *per se*, beyond quantum computation.

qPATHINT calculates propagation of quantum variables in the presence of shocks. Many real systems propagate in such contexts. qPATHINT is based on a classical-physics code, PATHINT, which has demonstrated its usefulness in several systems across several disciplines, including neuroscience and financial derivatives. This project deals specifically with two such systems, Statistical Mechanics of Neocortical Interactions (SMNI) and Statistical Mechanics of Financial Markets (SMFM).

Section 2 defines the PATHINT algorithm and its utility.

Section 3 gives a brief summary of the finance project further developed here for inclusion of quantum scales.

Section 4 reports new results calculating volatility of volatility in quantum spaces for a Eurodollar contract using qPATHINT. This is a similar calculation using PATHINT published in 2000 [1], and demonstrates the scope of qPATHINT.

Section 5 gives details of the qPATHINT code.

Section 6 describes some applications.

Section 7 is the Conclusion.

2. PATHINT

This section paraphrases previous papers by this author, including a recent paper [2]. It also closely follows Appendix B of another paper in progress by this author [3].

2.1. Path Integral in Stratonovich (Midpoint) Representation

Most suitable for examining discretization issues in time-dependent nonlinear systems, the path integral in the Feynman (midpoint) representation is [4–6] (N.b. $g^{\dagger}$ in DM implies a prepoint evaluation.) Unless stated otherwise, the Einstein summation convention is used for repeated indices to signify summation; bars $|\ldots|$ imply no summation.

$$P[M_t|M_{t_0}]dM(t) = \int\ldots\int DM \exp\left(-\min\int_{t_0}^{t} dt' L\right)\delta\big(M(t_0)=M_0\big)\delta\big(M(t)=M_t\big)$$

$$DM = \lim_{u\to\infty}\prod_{\rho=1}^{u+1} g^{\dagger 1/2}\prod_{G}(2\pi\theta)^{-1/2}dM_{\rho}^{G}$$

$$L(\dot{M}^G, M^G, t) = \frac{1}{2}(\dot{M}^G - h^G)g_{GG'}(\dot{M}^{G'} - h^{G'}) + \frac{1}{2}h^G_{;G} + R/6 - V$$

$$\dot{M}^G(t) \to M^G_{\rho+1} - M^G_{\rho}, M^G(t) \to \frac{1}{2}(M^G_{\rho+1} + M^G_{\rho}), [\ldots]_{,G} = \frac{\partial[\ldots]}{\partial M^G}$$

$$h^G = g^G - \frac{1}{2}g^{-1/2}(g^{1/2}g^{GG'})_{,G'}, h^G_{;G} = h^G_{,G} + \Gamma^F_{GF}h^G = g^{-1/2}(g^{1/2}h^G)_{,G}$$

$$g_{GG'} = (g^{GG'})^{-1}, g = \det(g_{GG'})$$

$$\Gamma^F_{JK} \equiv g^{LF}[JK, L] = g^{LF}(g_{JL,K} + g_{KL,J} - g_{JK,L})$$

$$R = g^{JL}R_{JL} = g^{JL}g^{JK}R_{FJKL}$$

$$R_{FJKL} = \frac{1}{2}(g_{FK,JL} - g_{JK,FL} - g_{FL,JK} + g_{JL,FK}) + g_{MN}(\Gamma^M_{FK}\Gamma^N_{JL} - \Gamma^M_{FL}\Gamma^N_{JK}) \tag{1}$$

2.2. Path Integral in Ito (Prepoint) Representation

For conditional probability distributions or for wave functions, the Ito development is in the prepoint representation:

$$P[M_t|M_{t_0}]dM(t) = \int \dots \int DM \exp\big(-\min \int_{t_0}^{t} dt' L\big)\delta\big(M(t_0) = M_0\big)\delta\big(M(t) = M_t\big)$$

$$DM = \lim_{u\to\infty} \prod_{\rho=1}^{u+1} g^{1/2} \prod_G (2\pi\Delta t)^{-1/2} dM^G_\rho$$

$$L(\dot{M}^G, M^G, t) = \frac{1}{2}(\dot{M}^G - g^G)g_{GG'}(\dot{M}^{G'} - g^{G'}) + R/6$$

$$\dot{M}^G(t) \to M^G_{\rho+1} - M^G_\rho, M^G(t) \to M^G_\rho$$

$$g_{GG'} = (g^{GG'})^{-1}, g = \det(g_{GG'}) \tag{2}$$

The diagonal diffusion terms are $g^{|GG|}$ and the drift terms are g^G. No-constant diffusions terms add terms to the drifts. A Riemannian-curvature potential $R/6$ arises for dimension > 1 in the midpoint Stratonovich/Feynman discretization.

2.3. Path-Integral Riemannian Geometry

The midpoint derivation derives a Riemannian geometry with a metric defined by the inverse of the covariance matrix

$$g_{GG'} = (g^{GG'})^{-1} \tag{3}$$

and where R is the Riemannian curvature

$$R = g^{JL}R_{JL} = g^{JL}g^{JK}R_{FJKL} \tag{4}$$

The Ito prepoint discretization gives a simpler algebraic form,

$$M(\bar{t}_s) = M(t_s)$$

$$L = \frac{1}{2}(dM^G/dt - g^G)g_{GG'}(dM^{G'}/dt - g^{G'}) - V \tag{5}$$

but the Lagrangian L is useful only in the weak-noise limit. This means that finer meshes are often required.

2.4. Three Approaches Are Mathematically Equivalent

Three basic different approaches are mathematically equivalent:

(a) Fokker-Planck/Chapman-Kolmogorov partial-differential equations
(b) Langevin coupled stochastic-differential equations
(c) Lagrangian or Hamiltonian path-integrals

The path-integral approach is particularly useful to precisely define intuitive physical variables from the Lagrangian L in terms of its underlying variables M^G:

$$\text{Momentum}: \ \Pi^G = \frac{\partial L}{\partial(\partial M^G/\partial t)}$$

$$\text{Mass}: \ g_{GG'} = \frac{\partial L}{\partial(\partial M^G/\partial t)\partial(\partial M^{G'}/\partial t)}$$

$$\text{Force}: \ \frac{\partial L}{\partial M^G}$$

$$F = ma: \ \delta L = 0 = \frac{\partial L}{\partial M^G} - \frac{\partial}{\partial t}\frac{\partial L}{\partial(\partial M^G/\partial t)} \tag{6}$$

Differentiation of noisy systems can introduce more noise. Integration is inherently a smoothing process, and the path-integral often gives superior numerical performance.

2.5. Stochastic Differential Equation (SDE)

The Stratonovich (midpoint discretized) Langevin equations can be analyzed in terms of the Wiener process dW^i, which can be rewritten in terms of Gaussian noise $\eta^i = dW^i/dt$ if care is taken in the limit.

$$dM^G = f^G\big(t, M(t)\big)dt + \hat{g}_i^G\big(t, M(t)\big)dW^i$$

$$\dot{M}^G(t) = f^G\big(t, M(t)\big) + \hat{g}_i^G\big(t, M(t)\big)\eta^i(t)$$

$$dW^i \to \eta^i dt$$

$$M = \{M^G; G = 1, \ldots, \Lambda\}$$

$$\eta = \{\eta^i; i = 1, \ldots, N\}$$

$$\dot{M}^G = dM^G/dt$$

$$< \eta^j(t) >_\eta = 0, < \eta^j(t), \eta^{j'}(t') >_\eta = \delta^{jj'}\delta(t - t') \tag{7}$$

η^i represents Gaussian white noise.

2.6. Partial Differential Equation (PDE)

The Fokker-Planck, or Chapman-Kolmogorov, partial differential equation is:

$$P_{,t} = \frac{1}{2}(g^{GG'}P)_{,GG'} - (g^G P)_{,G} + VP$$

$$P = < P_\eta >_\eta$$

$$g^G = f^G + \frac{1}{2}\hat{g}_i^{G'}\hat{g}_{i,G'}^{G}$$

$$g^{GG'} = \hat{g}_i^G \hat{g}_i^{G'}$$

$$(\ldots)_{,G} = \partial(\ldots)/\partial M^G \tag{8}$$

g^G replaces f^G in the SDE if the Ito (prepoint discretized) calculus is used to define that equation. If boundary conditions are added as Lagrange multipliers, these enter as a "potential" V, creating a Schrodinger-type equation.

2.7. Applications

Path integrals and PATHINT have been applied across several disciplines, including combat simulations [7], neuroscience [2,8–10], finance [1,2,11–15], and other nonlinear systems [16–18].

3. Statistical Mechanics of Financial Markets (SMFM)

3.1. Quantum Money

Quantum computing is here, and it will be applied to financial products, e.g., blockchains. It is reasonable to assume that soon there will be financial derivatives developed on these products. qPATHTREE and qPATHINT can calculate financial derivatives in these spaces. This is beyond simply using quantum computation of financial derivatives, since the space of the dependent variables themselves may live in quantum worlds [19–24].

3.2. Previous Applications — PATHINT

Options V are generally described by a portfolio Π over an underlying asset S. The real-world probability distribution of S often is critical to numerical details for trading. The asset is often hedged by trading the option V and a quantity Δ of the asset S.

$$d\Pi = \sigma\left(\frac{\partial V}{\partial S} - \Delta\right)dX + \left(\mu S\frac{\partial V}{\partial S} + \frac{1}{2}\sigma^2 S^2\frac{\partial^2 V}{\partial S^2} + \frac{\partial V}{\partial t} - \mu\Delta S\right)dt$$

$$\Gamma = \frac{\partial^2\Pi}{\partial S^2}, \Theta = \frac{\partial\Pi}{\partial t}, \mathrm{Y} = \frac{\partial\Pi}{\partial\sigma}, \rho = \frac{\partial\Pi}{\partial r} \tag{9}$$

The portfolio Π to be hedged is often considered to be "risk-neutral," if Δ is chosen such that $\Delta = \frac{\partial V}{\partial S}$.

While quite a few closed-form solutions exist for European options [25], where there is not early exercise. For American options — among the most popular options — there is no general closed form, and numerical calculations must be performed [26].

In the path-integral approach, first the probability "tree" for S is propagated forward in time until the expiration date T, branching out as extended S values develop. Then, marching back in time, at each time-node calculations of the Greeks above are developed, inserting changes in dividends, interest rates, changes in cheapest-to-deliver for baskets of bonds for options on bond futures, etc [1,27].

At each node a calculation is performed, comparing the strike price X to the price S at that node, and a decision is made, e.g., whether to exercise the option at that node, which determines the fair value of the option price V. To obtain the Greeks, extended derivatives of these Derivatives are calculated numerically by using values across branches and notes [1].

3.3. Aside: Application to Risk

Path integrals also have been applied to copula risk management. The approach to consider a basket of markets in their **dx** variables, each fit separately to real data, e.g., using a parameterized 2-tail exponential distribution. Then each market is transformed to a Gaussian distribution in their **dy** variables. The collection of Gaussians permits a multi-factor Gaussian to be developed from which meaningful considerations based on covariance can be based, e.g., for value at risk (VaR).

This gives a multivariate correlated process P in the dy variables, in terms of Lagrangians L and Action A,

$$P(dy) \equiv P(dy^1, ..., dy^N) = (2\pi dt)^{-\frac{N}{2}} g^{-\frac{1}{2}} \exp(-Ldt) \tag{10}$$

The Lagrangian L is

$$L = \frac{1}{2dt^2} \sum_{ij} dy^i g_{ij} dy^j \tag{11}$$

The effective action A_{eff}, presenting a "cost function" useful for sampling and optimization, is defined by

$$P(dy) = \exp(-A_{eff})$$

$$A_{eff} = Ldt + \frac{1}{2} \ln g + \frac{N}{2} \ln(2\pi dt) \tag{12}$$

3.3.1. Copula

The multivariate distribution in x-space is specified, including correlations, using

$$P(dx) = P(dy) \left| \frac{\partial\, dy^i}{\partial\, dx^j} \right| \tag{13}$$

where $\left| \frac{\partial dy^i}{\partial dx^j} \right|$ is the Jacobian matrix specifying this transformation. This yields

$$P(dx) = g^{-\frac{1}{2}} \exp\left(-\frac{1}{2} \sum_{ij} \left(dy^i_{dx}\right)^\dagger \left(g_{ij} - I_{ij}\right) \left(dy^j_{dx}\right) \right) \prod_i P_i(dx^i) \tag{14}$$

where $\left(dy_{dx}\right)$ is the column-vector of $\left(dy^1_{dx}, \ldots, dy^N_{dx}\right)$ expressed back in terms of their respective $\left(dx^1, ..., dx^N\right)$, $\left(dy_{dx}\right)^\dagger$ is the transpose row-vector, and $\left(I\right)$ is the identity matrix.

The Gaussian copula $C(dx)$ is defined by

$$C(dx) = g^{-\frac{1}{2}} \exp\left(-\frac{1}{2} \sum_{ij} \left(dy^i_{dx}\right)^\dagger \left(g_{ij} - I_{ij}\right) \left(dy^j_{dx}\right) \right) \tag{15}$$

Some additional work is performed to generate guaranteed stable numerical covariance matrices.

These calculations have been embedded as a middle layer in a program Trading in Risk Dimensions (TRD) [28]. An inner-shell is adaptively fit to incoming market data. An outer-shell uses Adaptive Simulated Annealing (ASA) [29] to fit historical data to parameterized trading-rules. A middle-shell risk-management middle-shell creates a three-shell recursive optimization/sampling/fitting algorithm. Portfolio-level distributions of copula-transformed multivariate distributions are generated by Monte Carlo samplings.

4. Volatility of Volatility of American Options

This section paraphrases a previous paper by this author [1].

4.1. SMFM Example of 2-Factor PATHINT

An example of a two-dimensional options model processed by PATHINT developed the volatility of volatility of options on Eurodollars, using 2-factor model developed by the author:

$$dS = \mu\, S\, dt + \sigma\, F(S, S_0, S_\infty, x, y)\, dz_S$$

$$d\sigma = \nu\, dt + \epsilon\, dz_\sigma$$

$$F(S, S_0, S_\infty, x, y) = S,\ S < S_0$$

$$F(S, S_0, S_\infty, x, y) = S^x S_0^{1-x},\ S_0 \leq S \leq S_\infty$$

$$F(S, S_0, S_\infty, x, y) = S^y S_0^{1-x} S_\infty^{x-y},\ S > S_\infty \tag{16}$$

where S_0 and S_∞ are selected to lie outside the data region used to fit the other parameters, e.g., $S_0 = 1/2$ and $S_\infty = 20$ for fits to Eurodollar futures.

Fig. 4 is a PATHINT example of a two-factor distribution evolved out to $T = 0.5$ year for $x = 0.7$.

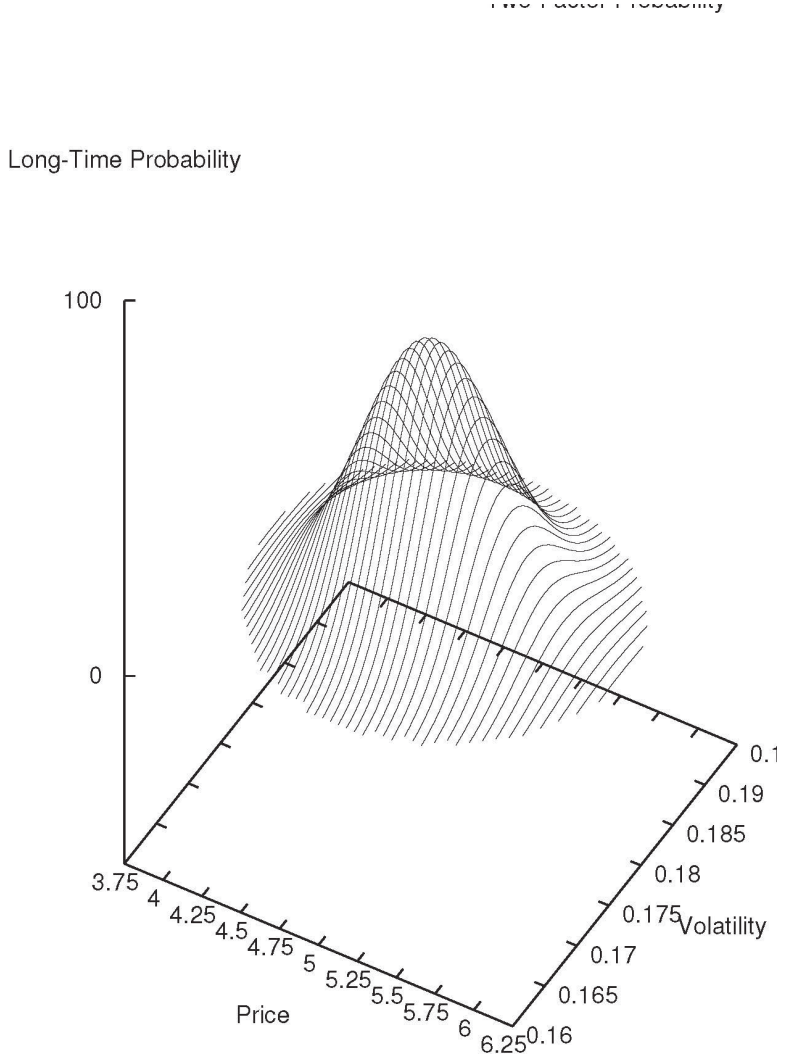

Figure 4 illustrates a two-factor distribution evolved out to $T = 0.5$ year for $x = 0.7$ [1].

4.2. SMFM Example of 2-Factor qPATHINT

qPATHINT was used to perform the similar calculations as were previously performed by PATHINT [1], except that whereas PATHINT propagates the probability, qPATHINT propogates the wave-function ψ and the kernels are normalized with $\psi^*\psi$. Since real variables were input, the output is the same for test sections of the code as previously reported using one-dimensional closed-form Black-Scholes [25] and numerical Cox-Ross-Rubenstein (CRR) codes [30]. Of course the output differs for the 2-dimensional volatility of volatility calculations, and there is no market data for quantum variables to test yet. This was another test for qPATHINT, illustrating that if complex variables were input (including real and imaginary non-zero values), then this can be processed by this code.

5. qPATHINT: Inclusion of Quantum Scales

5.1. PATHINT/qPATHINT Code

PATHINT was developed to numerically calculate the path integral, especially for serial changes in time, usually not approachable with standard Monte Carlo techniques.

qPATHINT was developed from the PATHINT C code of about 7500 lines of code. The C code run with the GCC C-compiler uses double complex variables instead of double variables. The code is

written for arbitrary N dimensions. The outline of the code is described here for classical or quantum systems, using generic coordinates q and x [11–13]:

This histogram procedure recognizes that the distribution (probabilities for classical systems, wave-functions for quantum systems) can be numerically approximated by sums of rectangles of height P_i and width Δq^i at points q^i.

5.1.1. Shocks

Many real-world systems propagate in the presence of continual "shocks":

future dividends
changes in interest rates
changes in asset distributions used in American options algorithms

5.1.2. PATHINT/qPATHINT Histograms

In the prepoint Ito discretization, using a one-dimensional system in variable x, the path-integral is written in terms of the kernel G, for each of its intermediate integrals, as

$$P(x;t+\Delta t) = \int dx' [g^{1/2}(2\pi\Delta t)^{-1/2}\exp(-L\,\Delta t)]P(x';t) = \int dx' G(x,x';\Delta t)P(x';t)$$

$$P(x;t) = \sum_{i=1}^{N} \pi(x-x^i)P_i(t)$$

$$\pi(x-x^i) = 1\,,\ (x^i - \frac{1}{2}\Delta x^{i-1}) \le x \le (x^i + \frac{1}{2}\Delta x^i);0\,,\ \text{otherwise} \tag{17}$$

This yields

$$P_i(t+\Delta t) = T_{ij}(\Delta t)P_j(t)$$

$$T_{ij}(\Delta t) = \frac{2}{\Delta x^{i-1} + \Delta x^i} \int_{x^i - \Delta x^{i-1}/2}^{x^i + \Delta x^i/2} dx \int_{x^j - \Delta x^{j-1}/2}^{x^j + \Delta x^j/2} dx' G(x,x';\Delta t) \tag{18}$$

T_{ij} is a banded matrix representing the Gaussian nature of the short-time probability centered about the (possibly time-dependent) drift.

Several projects have used this algorithm [9,18,27,31–33]. 2-dimensional codes were developed for Statistical Mechanics of Combat (SMC), Statistical Mechanics of Neocortical Interactions (SMNI) and Statistical Mechanics of Financial Markets (SMFM) [1,7,9].

5.1.3. Meshes For [q]PATHINT

Explicit dependence of L on time t also can be included. The mesh Δq^i, is strongly dependent on diagonal elements of the diffusion matrix, e.g.,

$$\Delta q^i \approx (\Delta t g^{|ii|})^{1/2} \tag{19}$$

The covariances develop a rectangular-ish underlying mesh. Fitting the data with integrals over the short-time distribution permits the use of coarser meshes than the corresponding stochastic differential equation(s) [31,34].

5.2. Lessons Learned From SMFM and SMNI

5.2.1. Broad-Banded Kernels Required

SMNI qPATHINT has emphasized the requirement of broad-banded kernels for oscillatory quantum states.

SMFM PATHTREE, and its derived qPATHTREE, is a different options code, based on path-integral error analyses, permitting a new very fast binary calculation, also applied to nonlinear time-dependent systems [14]. However, currently an SMFM [q]PATHTREE is only a binary tree with $J = 1$ and it cannot be effectively applied to quantum oscillatory systems [11–13].

5.2.2. SMFM qPATHINT With Serial Shocks

A University of California San Diego (UCSD) supercomputer resource is Comet.

Some N-dim qPATHINT runs for SMFM used a contrived N-factor model with the same 1-dimensional system cloned in all dimensions (each unit is a "double complex"):

D=1:imxall: 27 , jmxall: 7 , ijkcnt: 189
D=2:imxall: 729 , jmxall: 49 , ijkcnt: 35721
D=3:imxall: 19683 , jmxall: 343 , ijkcnt: 6751269
D=4:imxall: 531441 , jmxall: 2401 , ijkcnt: 1275989841
D=5:imxall: 14348907 , jmxall: 16807 , ijkcnt: 241162079949
D=6:imxall: 387420489 , jmxall: 117649 , ijkcnt: 45579633110361
D=7:imxall: 10460353203 , jmxall: 823543 , ijkcnt: 8614550657858229

The kernel size is $(IJ)^N$, where I = imxall, J = jmxall (= kernel band width), and kernel size = ijkcnt. This spatial mesh might change at each time slice.

A full set of Adaptive Simulated Annealing (ASA) [29] fits of classical SMNI to EEG data takes about 1000 hours of supercomputer CPUs; many such sets of runs are required to develop good models. Cost functions that include quantum processes will take even longer.

6. Applications

6.1. Quantum Money and Blockchains

Quantum computing is here, and in the near future it will be applied to financial products, e.g., blockchains. Soon financial derivatives will be developed on these products. qPATHINT can calculate financial derivatives in these spaces. The marketplace will determine traded variables:

6.2. Enhanced Security/Verification

Quantum currency cannot be cloned. Such currencies are candidates for efficient blockchains. Each “coin” has a unique identity [19,22,23,35]. There are issues about the decoherence time of such currency.

7. Conclusion

A summary of a the qPATHINT methodology is presented, including requirements for large kernel bands.

For financial markets the SMFM model has demonstrated it is faithful to experimental data, developing financial options using the classical PATHINT algorithm. qPATHINT similarly calculates quantum options with serial shocks on quantum money, evolving the quantum distribution of a quantum price variable, and calculating early exercise, marching back in time from the option maturity date. 2-dimensional calculations have been performed for Eurodollar volatility of volatility.

3-dimensional calculations have been shown to be feasible. This presents a rationale for this particular quantum path-integral algorithm.

$Id: https://www.ingber.com/markets18_quantum_options.pdf 1.15 2018/08/12 15:30:03$

References

1. Ingber, L. High-resolution path-integral development of financial options. *Physica A* **2000**, *283*, 529–558. https://www.ingber.com/markets00_highres.pdf.
2. Ingber, L. Quantum Path-Integral qPATHINT Algorithm. *The Open Cybernetics Systemics Journal* **2017a**, *11*, 119–133. http://dx.doi.org/10.2174/1874110X01711010119.
3. Ingber, L. Quantum calcium-ion interactions with EEG. Technical Report Report 2018:QCIE, Lester Ingber Research, Ashland, OR, 2018. https://www.ingber.com/smni18_quantumCaEEG.pdf.
4. Langouche, F.; Roekaerts, D.; Tirapegui, E. Discretization problems of functional integrals in phase space. *Physical Review D* **1979**, *20*, 419–432.
5. Langouche, F.; Roekaerts, D.; Tirapegui, E. *Functional Integration and Semiclassical Expansions*; Reidel: Dordrecht, The Netherlands, 1982.
6. Schulman, L. *Techniques and Applications of Path Integration*; J. Wiley & Sons: New York, 1981.
7. Ingber, L.; Fujio, H.; Wehner, M. Mathematical comparison of combat computer models to exercise data. *Mathematical Computer Modelling* **1991**, *15*, 65–90. https://www.ingber.com/combat91_data.pdf.
8. Ingber, L. Statistical mechanics of neocortical interactions: Path-integral evolution of short-term memory. *Physical Review E* **1994**, *49*, 4652–4664. https://www.ingber.com/smni94_stm.pdf.
9. Ingber, L.; Nunez, P. Statistical mechanics of neocortical interactions: High resolution path-integral calculation of short-term memory. *Physical Review E* **1995**, *51*, 5074–5083. https://www.ingber.com/smni95_stm.pdf.
10. Ingber, L.; Nunez, P. Neocortical Dynamics at Multiple Scales: EEG Standing Waves, Statistical Mechanics, and Physical Analogs. *Mathematical Biosciences* **2010**, *229*, 160–173. https://www.ingber.com/smni10_multiple_scales.pdf.
11. Ingber, L. Path-integral quantum PATHTREE and PATHINT algorithms. *International Journal of Innovative Research in Information Security* **2016**, *3*, 1–15. https://www.ingber.com/path16_quantum_path.pdf.
12. Ingber, L. Evolution of regenerative Ca-ion wave-packet in neuronal-firing fields: Quantum path-integral with serial shocks. *International Journal of Innovative Research in Information Security* **2017b**, *4*, 14–22. https://www.ingber.com/path17_quantum_pathint_shocks.pdf.
13. Ingber, L. Options on quantum money: Quantum path-integral with serial shocks. *International Journal of Innovative Research in Information Security* **2017c**, *4*, 7–13. https://www.ingber.com/path17_quantum_options_shocks.pdf.
14. Ingber, L.; Chen, C.; Mondescu, R.; Muzzall, D.; Renedo, M. Probability tree algorithm for general diffusion processes. *Physical Review E* **2001**, *64*, 056702–056707. https://www.ingber.com/path01_pathtree.pdf.
15. Ingber, L.; Wilson, J. Statistical mechanics of financial markets: Exponential modifications to Black-Scholes. *Mathematical Computer Modelling* **2000**, *31*, 167–192. https://www.ingber.com/markets00_exp.pdf.
16. Ingber, L. Path-integral evolution of multivariate systems with moderate noise. *Physical Review E* **1995**, *51*, 1616–1619. https://www.ingber.com/path95_nonl.pdf.
17. Ingber, L. Data mining and knowledge discovery via statistical mechanics in nonlinear stochastic systems. *Mathematical Computer Modelling* **1998**, *27*, 9–31. https://www.ingber.com/path98_datamining.pdf.
18. Ingber, L.; Srinivasan, R.; Nunez, P. Path-integral evolution of chaos embedded in noise: Duffing neocortical analog. *Mathematical Computer Modelling* **1996**, *23*, 43–53. https://www.ingber.com/path96_duffing.pdf.
19. Aaronson, S.; Christiano, P. Quantum money from hidden subspaces. Technical Report arXiv:1203.4740 [quant-ph], MIT, Cambridge, MA, 2012.

20. Accardi, L.; Boukas, A. The quantum Black-Scholes equation. Technical Report arXiv:0706.1300 [q-fin.PR], U di Roma Torvergata, Rome, 2007.
21. Baaquie, B.; Coriano, C.; Srikant, M. Quantum mechanics, path integrals and option pricing: Reducing the complexity of finance. Technical Report arXiv:cond-mat/0208191 [cond-mat.soft], National U Singapore, Singapore, 2002.
22. Jogenfors, J. Quantum bitcoin: An anonymous and distributed currency secured by the no-cloning theorem of quantum mechanics. Technical Report arXiv:1604.01383 [quant-ph], Linkoping U, Linkoping, Sweden, 2016.
23. Meyer, K. Extending and simulating the quantum binomial options pricing model. Technical Report Thesis, U Manitoba, Winnipeg, Canada, 2009. http://hdl.handle.net/1993/3154.
24. Piotrowski, E.; Schroeder, M.; Zambrzycka, A. Quantum extension of European option pricing based on the Ornstein-Uhlenbeck process. *Physica A* **2005**, *368*, 176–182.
25. Black, F.; Scholes, M. The pricing of options and corporate liabilities. *The Journal of Political Economy* **1973**, *81*, 637–659.
26. Hull, J. *Options, Futures, and Other Derivatives, 4th Edition*; Prentice Hall: Upper Saddle River, NJ, 2000.
27. Ingber, L.; Wilson, J. Volatility of volatility of financial markets. *Mathematical Computer Modelling* **1999**, *29*, 39–57. https://www.ingber.com/markets99_vol.pdf.
28. Ingber, L. Trading in Risk Dimensions. In *The Handbook of Trading: Strategies for Navigating and Profiting from Currency, Bond, and Stock Markets*; Gregoriou, G., Ed.; McGraw-Hill: New York, 2010; pp. 287–300.
29. Ingber, L. Adaptive Simulated Annealing (ASA). Technical Report Global optimization C-code, Caltech Alumni Association, Pasadena, CA, 1993. https://www.ingber.com/#ASA-CODE.
30. Cox, J.; Ross, S.; Rubenstein, M. Option pricing: A simplified approach. *Journal Financial Economics* **1979**, *7*, 229–263.
31. Wehner, M.; Wolfer, W. Numerical evaluation of path-integral solutions to Fokker-Planck equations. I. *Physical Review A* **1983a**, *27*, 2663–2670.
32. Wehner, M.; Wolfer, W. Numerical evaluation of path-integral solutions to Fokker-Planck equations. II. Restricted stochastic processes. *Physical Review A* **1983b**, *28*, 3003–3011.
33. Wehner, M.; Wolfer, W. Numerical evaluation of path integral solutions to Fokker-Planck equations. III. Time and functionally dependent coefficients. *Physical Review A* **1987**, *35*, 1795–1801.
34. Ingber, L. Statistical mechanical aids to calculating term structure models. *Physical Review A* **1990**, *42*, 7057–7064. https://www.ingber.com/markets90_interest.pdf.
35. Bartkiewicz, K.; Cernoch, A.; Chimczak, G.; Lemr, K.; Miranowicz, A.; Nori, F. Experimental quantum forgery of quantum optical money. Technical Report arXiv:1604.04453v1 [quant-ph], Adam Mickiewicz University, Poznan, Poland, 2016.